JOURNAL OF PROPULSION AND POWER
Vol. 19, No. 1, January–February 2003

Optical Fouling of the RB199 Pyrometer

Clive Kerr* and Paul Ivey†
Cranfield University, Cranfield, England MK43 OAL, United Kingdom

The Turbo-Union RB199 aeroengine, which powers the Panavia Tornado aircraft, has two pyrometers installed to measure and control turbine blade temperature. The utilization of pyrometry and its installation, together with system configuration, for this in-flight application are described. The most important issue with pyrometry for in-service use is the deposition of particulates, or optical fouling, of the system's lens. The flowfield and particle trajectories in the RB199 pyrometer purge air design are investigated together with an analysis of the deposits that constitute the fouling of the pyrometer lens. It will be shown that the predominant flow feature within the purging system is a swirl pattern that develops at the mouth of the still tube. This feature has the ability to draw contaminant particles into the still tube and, thus, significantly increase the likelihood of particle deposition onto the lens resulting in optical fouling of the instrument's optics.

Introduction

OPTICAL pyrometry is a noncontact method of surface temperature measurement that is employed to measure turbine blade temperature. This technique does not perturb the surface of the target material, or surrounding medium, and operates by collecting thermal radiation from a defined target spot on the turbine blades, which is optically transferred to a detector, to produce an output signal proportional to the radiance emitted from the blades. This study describes the in-service use of pyrometry and investigates the associated fouling of the pyrometer lens on the Turbo-Union RB199 aeroengine. Presented within this paper will be the results of numerical modeling of the RB199 pyrometer purge air system, using computational fluid dynamics, which illustrates the fouling mechanism and subsequent particle deposition onto the pyrometer lens.

In-Flight Pyrometer System

Pyrometer Installation

Each RB199 is fitted with two single-band pyrometers, an example of which is presented in Fig. 1, which are designed and manufactured by Land Infrared of Dronfield, England. The two pyrometers are installed at the 4 and 5 o'clock positions viewing the pressure surface of the engine's single-stage IPT blades. Each pyrometer has a direct viewing installation, which provides a direct line of sight of its target as depicted in Fig. 2, with only the optic head of the instrument located on the turbine casing, then with a fiber optic light guide extracting the optical signal. The sight tubes of the pyrometers are cylindrically shaped and mounted with its forward end projecting through an aperture in the engine casing.

System Configuration

The RB199 pyrometer is composed of the following four distinct elements.

1) A sight tube assembly accommodates the optic interface between the lens and the fiber optic light guide, to define the target spot and collect the emitted thermal radiation and the purge air system to maintain deposit free optics.

2) The fiber optic light guide transmits this thermal radiation from the probe to the detector.

3) The detector, sensitive to a prescribed spectral range, produces an output proportional to radiance.

4) The last element is an electronics module for the necessary signal conditioning.

From an optical point of view, the RB199 pyrometer sight tube probe (Fig. 3) consists of a single lens system, held in position by a metal casing, which defines a target area on the pressure surface of the IPT blades from which radiation is collected. The target size is approximately 8.3 mm in diameter.

Single-band pyrometers are installed onto the turbine casing. Because single-band pyrometers sense only radiation from within a single specified waveband, this type of system more easily permits the bandwidth and signal-to-noise ratio performance necessary to track the temperature profile around rotating bodies such as the turbine blades. The spectral bandwidth for the RB199 system is considered to be 0.6–1.1 μm.

In view of the arduous environment, the selection of materials for the optical elements is important. The RB199 pyrometer lens is constructed from sapphire, a material that offers high resistance to thermal shock and chemical attack combined with good transmission for the spectral sensitivity range of the silicon detector. The sapphire lens is brazed into the 42% nickel (balance Fe) holder (nickel plated) with a silver/copper eutectic material. Before being brazed, the lens has molybdenum sintered to the periphery, which is then nickel plated.

The installed systems employ a fiber optic light guide to transfer the thermal radiation signal to the pyrometer detector. Fiber optic light guides were introduced so that the detector and electronics could be located in an area with less severe ambient temperature compared to that of the sight tube on the turbine casing. This has the result of minimizing the vibration and cooling requirements for the detector. In the case of the RB199 pyrometer installation, the length is the light guide is approximately 1 m.

At the end of the light guide there is a detector unit, which sits on the oil cooler, containing the visible-near infrared silicon detector, two thermistors, and a number of resistors. All of these electronic components have a temperature capability of approximately 200°C and are housed in a small, hermetically sealed, stainless steel casing with a high-temperature firewall type connector. Every pyrometer's detector unit is tested at 190°C. The purpose of the detector is to receive and convert the thermal radiant energy to an electrical signal suitable for transmission to the signal processor. The detector is the key component in the pyrometer because it is the means by which the incident radiation is converted to a measurable parameter. The silicon diode is selected as the detector of choice for several reasons. First, silicon diodes have the fast response time required to detect the temperature profile of individual blades on the rotor. Second, the

Received 29 April 2002; revision received 6 September 2002; accepted for publication 15 September 2002.

*Research Engineer, School of Engineering, Gas Turbine Instrumentation Group; c.i.v.kerr.1998@cranfield.ac.uk.

†Senior Lecturer, School of Engineering, Head of Turbomachinery; p.c.ivey@cranfield.ac.uk.

Fig. 1 RB199 pyrometer.

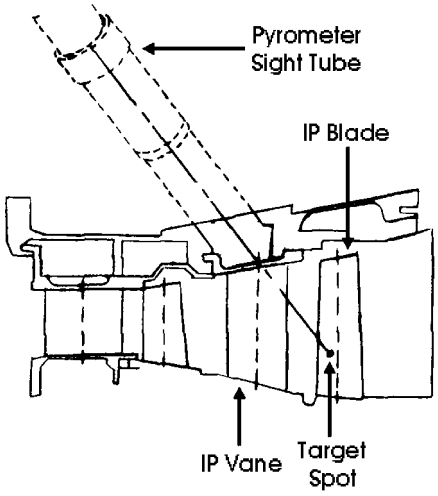

Fig. 2 Direct viewing installation.

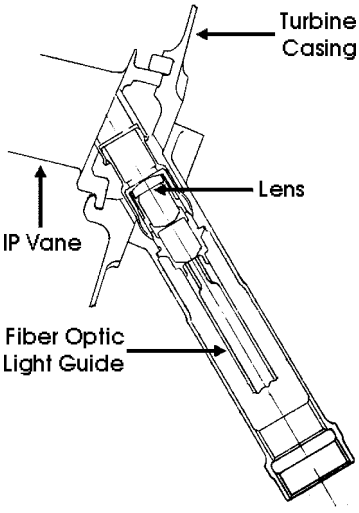

Fig. 3 RB199 pyrometer mounting.

spectral response of the silicon detector is in a region where there is minimal absorption and emission from the hot gases and products of combustion.[1]

An important consideration for any in-flight pyrometer is the lower temperature limit of the system, due to the spectral characteristics of the silicon detector, below which the instrument will not respond. This lower temperature limit means that during engine startup there would be no output signal, and a second method of temperature measurement, such as the addition of a thermocouple, has to be employed to monitor the engine at low-power settings. This dual system would use the pyrometer signal when the engine was in a steady state and at high-power, high-temperature performance points and employ the thermocouple signals during engine transient conditions, particularly during startup and relight. By the use of this approach, both technologies would complement each other, resulting in an optimum system of temperature control. Such a system is employed on the Turbo-Union RB199 aeroengine.

Instrument Function

The ability to make accurate blade temperature measurements offers the potential to increase performance by allowing the engine to operate closer to the temperature limit of the turbine blades. In addition, direct measurement of the turbine blades ensures that this temperature limit is not exceeded because this would reduce blade life drastically. According to Rohy et al.,[2] a few minutes of operation at over-temperature conditions can result in dramatic reductions in blade life and potentially catastrophic failure of the turbine. A significant fault found on nozzle vanes and turbine blades in the RB199 is burning.[3] This was generally the result of either hot spots, that is, a poor combustion chamber exit temperature profile, or ineffective blade cooling, for example, from blocking of cooling passages by abraded seal material.[3]

High-temperature limiting through pyrometry is used on the RB199 aeroengine.[4] This temperature control function limits the turbine blade temperature (TBT) to a predetermined value, and if the TBT exceeds this datum, then engine fuel flow is reduced, thus ensuring that the TBT remains within its limits. According to Wheatley,[5] the RB199 became the first production aeroengine to use pyrometry for primary engine control. The installation of two single-band pyrometers (Fig. 1) viewing the engine's single-stage IPT together with an exhaust gas temperature thermocouple provide the necessary signals to the engine control unit. The engine control unit then regulates fuel to the combustor because the RB199 engine is turbine entry temperature (TET) limited (maximum TET of 1590 K) (Ref. 6).

Fouling of the Pyrometer Lens

Problem with Optical Fouling

The RB199 pyrometer has only one optical surface, namely, the lens, exposed to the turbine environment (Fig. 3). This means that particulates, such as soot and sand, can deposit on the lens and act as a filter by absorbing some of the thermal radiation from the blades. This results in an output signal that is representative of a lower temperature than the actual blade temperature due to the measurement errors introduced by fouling. For the control application of high-temperature limiting, this would permit higher turbine temperature operation resulting in blade temperatures in excess of their intended limits and, thus, shortening blade life. Therefore, the pyrometer lens must be maintained free from deposits if accurate temperature readings are to be maintained. It is acknowledged that the optical contamination of the lens is the major source of error in the use of pyrometry temperature measurement in gas turbines.[7] Kirby[8] further reinforces this point by stating that "lens contamination is of crucial importance since it constitutes a fail-dangerous error mode."

Pyrometer Purge Air System

The provision of a purge air system to the RB199 pyrometer attempts to reduce the likelihood of any contaminants depositing onto its lens. The essence of the purge air system is to maintain a positive pressure flow through the sight tube to prevent combustion gases with suspended particles from entering the pyrometer and contaminating the lens. This is accomplished by introducing purge air, bled from the compressor, down the sight tube to prevent both the buildup of contaminants on the exposed system optics and to prevent particles in the turbine gas stream from coming in contact with the lens.

According to Sellers et al.,[9] the purge air arrangement is probably the most critical aspect of the pyrometer system for use in engine

control with the success of the system being driven by the cleanliness of the lens surface. Thus, it is the reliability of the purge air system, for the limitation or control of optic contamination, that not only has a significant impact on the turbine blade temperature signals and, hence, blade life but also for engine on-wing times as a result of the cleaning time intervals for the instrument. The goal of purge design is to obtain the minimal level of lens particle deposition for a given operating cost, in terms of purge air mass flow, for the specific operating pressure conditions and allowable instrument size envelope.

Before 1992, the RB199 pyrometer purge air system utilized the air scrubbing configuration in Fig. 4. The air scrubbing approach utilizes the layer attachment or Coanda effect whereby the purge airflow is directed over the lens surface to form a barrier to prevent any particulates penetrating the sight tube from coming into contact with the lens.[7] As the purge air flows over the lens, it tends to scrub across its surface, and any particles on the lens will be reentrained. The purge must be controlled to maintain an adequate flow velocity to ensure that any particles that are removed from the lens remain entrained and are carried outwardly away from the optics. An important advantage of this configuration is that the scrubbing action permits the removal of ignition phase deposits that may form during engine startup.[10] Also any particles that deposit as the aeroengine shuts down, due to gravitational settling, for example, are then removed when the purge system begins to operate with engine startup. However, Hayden et al.[11] acknowledged two principal disadvantages with the scrubbing approach: First, any particles in the purge air itself are brought to the lens, thus, increasing the likelihood of deposition. Second, although the scrubbing action can remove large particles, the technique experiences difficulty in removing submicrometer particles or large sticky particles already deposited.

There were a lot of problems with the air scrubbing configuration during in-service use, and there were even instances of over-fueling and, thus, burning of blades due to lens fouling or sooting. A star-shaped deposit or crust was found to be baked onto the outer surface of the lens with a deeper section of deposits in the center, as shown in Fig. 5. Note that, the darker the shading in Fig. 5, the deeper are the deposits. Pyrometer operation was limited to only 25 h after which the lens had to be cleaned, using a metal cleaner and a lint free cloth, and the pyrometer recalibrated. Note that one of the most critical aspects in developing a purge design is the imposed space restriction, dictated by envelope size, and in the case of the RB199 installation, this played a major role in compromising the purge geometry and, hence, its effectiveness. Because of the poor operational performance of the air scrubbing design, given the tight size envelope for the purge geometry, a redesign of the purge system was undertaken.

After 1992, the newly redesigned purge air system entered service employing the still tube configuration. This is essentially an air curtain design approach whereby the addition of a still tube extension in front of the lens, illustrated in Fig. 6, establishes a barrier that prevents any contaminants from entering the sight tube. This tube has the function of establishing a still region in front of the lens. The principal advantage of the still tube configuration is the reduced probability of the lens being contaminated by any particles in the purge air itself because the airflow does not make direct contact with the lens.[7]

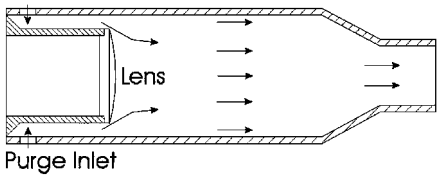

Fig. 4 Air scrubbing configuration.

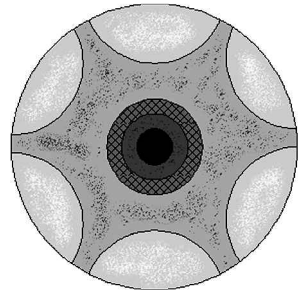

Fig. 5 Star-shaped deposit on lens of air scrubbing configuration.

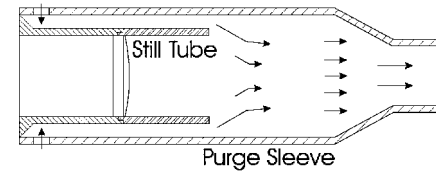

Fig. 6 Still tube configuration.

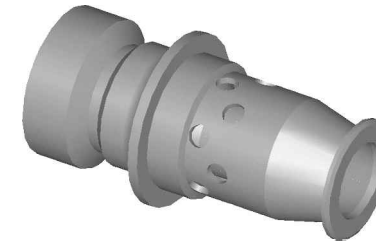

Fig. 7 RB199 pyrometer purge air system.

Two disadvantages emerge from this approach: First, particles may become trapped and then accumulate in the dead air zone between the lens and air curtain.[11] Second, there is no mechanism for removing any particles that may settle on the surface of the lens after the aeroengine shuts-down, excluding cleaning during routine maintenance.[7]

The current RB199 pyrometer purge air system is a short, multiple air inlet design as shown in Fig. 7. The purge air is fed from a plenum surrounding the purge sleeve through two rows of six inlets, which are offset by an angle of 30 deg and with each inlet circular in shape with a diameter of 2.70 mm. The multiple inlet design is, of course, to provide an adequate volume of purge flow but does add to the complexity of design and manufacture. The most noticeable design parameters for this purge system are a still tube length-to-diameter ratio L/D of 3:1, a distance of 38 mm from lens face to purge outlet and a path length of approximately 17 mm from purge inlets to outlet. In-service experience from this still tube configuration has shown negligible deposits over 150 h operation, and the pyrometer system is no longer a maintenance burden because it now lies within normal operational maintenance intervals for the RB199 aeroengine. The in-service experience of the purging systems using the still tube has proved so good, as contrasted to the old air scrubbing design, that personnel within certain air forces call the system the "self-cleaning pyrometer." However, the unit is not self-cleaning; it merely has an exceptionally improved performance. It will be shown later that there still remains a degree of optical contamination and that there is scope for further design improvements.

Sources of Contamination

There are two sources of lens fouling within any pyrometer purge air system.[7] The first and the most obvious is gas stream particles in the turbine chamber that enter through the sighting aperture of the purge sleeve. It is this source of contamination, termed turbine chamber penetration, that the purge air system is employed to minimize if not prevent. The operating mechanism of the purge system is to provide and maintain a positive pressure through the sight tube to prevent particulates in the turbine gas stream from penetrating the sight tube and reaching the lens. Such penetrating particles typically have high inertia and, thus, the purge airflow must be adequate to redirect these contaminants back around and down the sight tube to reenter the turbine chamber.

The other contributing factor to lens fouling is more subtle, yet just as significant; the fact that the source of purge air is bled from the compressor means that particles are present in the purge airflow itself. This second source of contamination, termed purge air

deposition, whereby particles from the purge air can deposit, is sometimes easily overlooked in some systems. Compressor bleed air is used as the supply for the pyrometer purge system, and it is usually laden with particulates that originate from the surrounding atmosphere ingested by the engine. For example, any sand that reaches the pyrometer will probably be in a molten state and, thus, be sticky so that it adheres to the lens and will then further attract other particles, increasing the accumulation.

Analysis of Lens Deposits

Pyrometer lens deposits can be categorized as either engine derived, including combustion products and mechanically abraded particles, or ingested. To gain a perspective on the type of particles that may find their way through the RB199 engine to deposit on the pyrometer lens, a literature survey was conducted on appropriate sources of contaminant particles, and a scanning electron microscope (SEM) analysis was carried out on several samples of actual lens deposits from in-service RB199 pyrometers.

Hayden et al.[11] conducted field particle sampling of the compressor line, purging source, and turbine chamber for a pyrometer operating on a turbine engine mounted on an engine test stand. They found that the particle mass concentration of compressor air ranged from 0.03 to 0.22 mg/m^3 depending on engine condition and that SEM examination of filter samples for the turbine chamber confirmed that most of the particles were soots. These soots had a mass median diameter of 0.13–0.25 μm with geometric standard deviation from 1.65 to 2.0. Soot is a result of incomplete combustion and is formed in fuel rich regions of the flame.[12] The amount of soot is produced from the combustion process is dependent on many factors, including mixture fraction, fuel–air mixing, temperature, and residence time in the soot production and consumption zones.[12] There is also the belief that large quantities of soot are produced at takeoff conditions, where the high pressures encourage soot formation. Analysis of the soot found in exhaust gases shows that it consists mostly of carbon (96%) and a mixture of hydrogen, oxygen, and other elements.[13]

Brocklehurst[12] reported that as soot ages its character changes and that collisions lead to the formation of chain agglomerates. Such soot aggregates are made up of primary particles that are virtually monodisperse with primary particles in the size range of 40–50 nm. Koylu et al.[14] found that the maximum primary particle size is 60 nm. Their experiments also showed that the number of primary particles in each agglomerate varies between 30 and 1800 primary particles. This can lead to large variations in size estimates for soot particles depending on the measurement technique used. Smoke particulate data measured as part of the Aerotrace program, as reported by Smedley,[15] had average particle diameter 55–65 nm. Investigations into the spectral transmission properties of engine soot have revealed that its absorption characteristics are nongray.[16] Therefore, if soot is allowed to accumulate on the pyrometer lens, both single-band and two-color measurements will be affected. Fisher and Lewis's data was collected from a pyrometer lens with no purge air flowing.[16] Note that the magnitude of the error from the deposition of soot onto a pyrometer lens is a function of the purge air system design, lens temperature, engine operating condition, and exposure time.

Myhre et al.[17] noted that mechanically abraded particles and even some submicrometer oil mists are present in the compressor flow that is used for pyrometer purging. In terms of ingested particulates that may find their way to a pyrometer lens, sand appears to be the most appropriate suspect especially for military operations in desert regions. A number of desert samples were collected and analyzed by Sage[18] during field trials and from places where engines were badly eroded in service, for example, South Arabia and Libya. It was found that sand particles range from about 50 to 1000 μm and that most natural sands have very little material less than 50 μm. Yet, it must be remembered that the size of particle that will reach the engine intake depends on the type of vehicle and its mode of operation. Sand that is blown by the wind or moved by water tends to have sharp corners removed and most of the desert and beach samples of Sage[18] were found to have subangular or rounded grains. Moorcroft[19] also conducted a particle analysis of sand using 5 Algerian desert sands and 10 further samples from Saudi Arabia. Based on the samples, the Algerian and Saudi Arabian desert sands were found, overall, to have similar particle size distributions. It was found that 100–300 μm was the size range in which sand will become airborne and cause most erosion within the engine. Additionally, the desert sands from both Algeria and Saudi Arabia were found to be rounded in shape.

Several samples of the lens's deposits were taken using cotton wool swabs during field sampling of in-service RB199 pyrometer systems. These samples were mounted on specimen plates and coated in a gold/palladium (80/20) film (Fig. 8) to produce a conductive sample for analysis under an SEM together with nondispersive x-ray analysis attachment to determine both the particle characteristics and chemical constituents of the deposits. Figures 9a–9c present

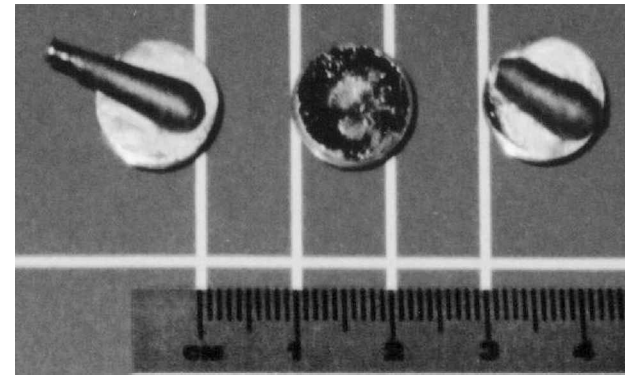

Fig. 8 SEM specimens.

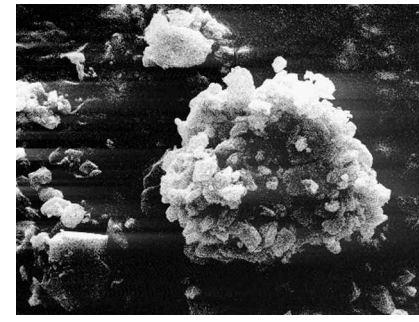

a)

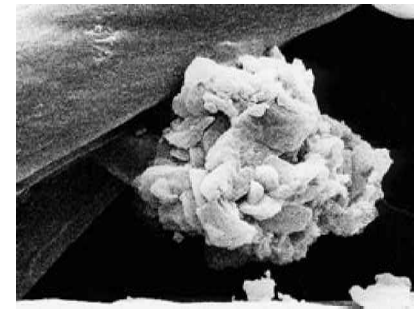

b)

c)

Fig. 9 SEM photographs of lens deposits.

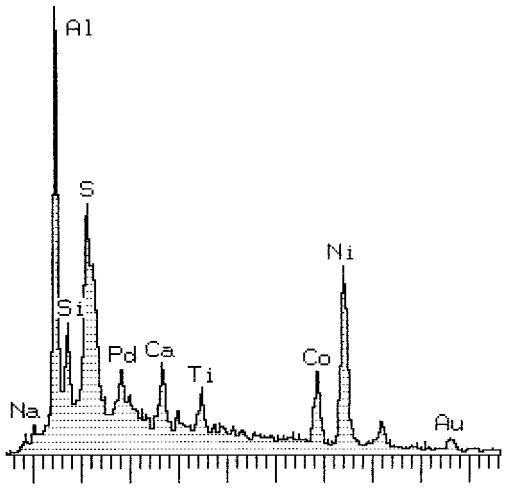

Fig. 10 Chemical composition of lens deposits.

SEM photographs of the type of particles that are found deposited on the RB199 pyrometer lens. The deposits in Figs. 9a and 9b appear crystalline in nature and are composed of much smaller particles (0.5–3 μm) forming an agglomerate (10–15 μm). The particle in Fig. 9c is sand (SiO_2) with a diameter of approximately 50 μm. Note that this particle has a number of smaller deposits adhering to its surface and may illustrate the sticking or attractive forces between the deposits due to the high temperature experienced at the surface of the pyrometer lens (approximately 500°C).

The deposit specimens were also analyzed under the SEM using nondispersive x-ray analysis attachment, an example of which is shown in Fig. 10, to determine the constituents that represent the optical fouling on the lens. Note that the SEM used for this study did not have the capability to identify carbon (C), nitrogen (N), or oxygen (O) due to the weak signals that must be detected from these elements and because their signals are further weakened due to the gold/palladium (Au/Pd) film on the deposits and the protective beryllium filter in front of detector of the SEM. With this in mind, the major constituents appear to be aluminium (Al), which is used as a turbine surface passivation coating; silicon (Si), from sand (SiO_2) ingestion; sulphur (S), from the combustion of the fuel source; calcium (Ca), which from experience is from calcium sulphate ($CaSO_4$) deposits; and nickel (Ni), from nickel oxide, which is essentially burnt turbine blade material. There were also trace amounts of sodium (Na), from a sodium salt whose origin is unknown but possibly sodium sulphate due to the fuel, and titanium (Ti), which is unusual but is quite possibly from the compressor blading because compressor bleed air is used as the source of purging. These results are comparative to those conducted by Rosemount (see Ref. 11), whose data showed the presence of particles that were basically dirt from the Earth such as Si, Ca, S, and Al and also engine generated particles of Ni, Cr, Fe, and Ti. It must be remembered that the Au and Pd shown in Fig. 10 is due to the mix used as a film to produce a conductive sample.

Modeling of the Purge Air System

Computational Fluid Dynamics Modeling Setup

Numerical analysis of the RB199 pyrometer purge air system was conducted through computational fluid dynamics (CFD) modeling to provide a deeper insight and understanding of the purging process. The solver chosen for the numerical study was FLUENT 5, which is a commercially available finite volume code produced by Fluent, Inc. The GAMBIT program, which is a part of the FLUENT package, was the preprocessor used for geometry modeling and mesh generation. Through the use of GAMBIT, the RB199 purge air system volume was meshed using an unstructured tetrahedral grid. This approach was chosen because the flow problem being solved involved a rather complex internal geometry, especially with the system's 12 inlets and compact flow domain. The other major motivation for using an unstructured grid, employing tetrahedral cells, was the reduced mesh generation time. A mesh-independence test was conducted whereby a series of grids, with significantly differing resolutions, were run until an acceptable balance of accuracy and computational complexity was achieved. For the RB199 purge air system model, the resultant mesh contained in the region of 240,000 cells.

Table 1 Flow specification for modeling

Location	Pressure, kPa	Temperature, K
	Cruise	
Purge inlets	900	580
Purge outlet	620	1125
	Maximum thrust	
Purge inlets	1300	650
Purge outlets	905	1330

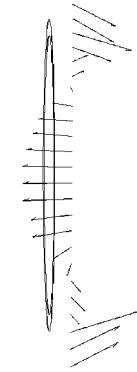

Fig. 11 Flow redirection at mouth of still tube.

There were two sets of engine representative boundary conditions chosen for the numerical simulations, those being operation at cruise and at maximum thrust, as specified in Table 1. Within Fluent, several test runs of the model was conducted to find the appropriate schemes and settings to use, thus facilitating the constraints of computational cost vs accuracy. For the RB199 model the three-dimensional, steady-state, segregated solver was used. The RNG k–ε turbulence model provided the best balance in terms of run time with a turbulence intensity of 10% and associated length scale of 0.1 mm together with the SIMPLE method for pressure–velocity coupling. The CFD modeling process and settings were experimentally validated through laser Doppler anemometry measurements with an actual purge air system manufactured from perspex.[20]

Analysis of Flowfields

Solutions were acquired for the RB199 pyrometer purge air model at cruise and maximum thrust engine conditions to discover the important flow features that develop within this configuration. The primary features to identify within the study of purge system flowfields are any recirculations within the sight tube that may draw in contaminants or otherwise enhance particle deposition.

Analysis of the velocity vectors for the flowfield within the purge system identified that there is significant swirl or recirculation in front of the still tube mouth, as illustrated in Fig. 11. Although Fig. 11 only shows the swirl effect in a two-dimensional cross section, this recirculation is, of course, a three-dimensional circumferential effect. This swirl that develops can be seen to converge a distance in front of the still tube mouth where a portion of the purge air undergoes a 180-deg direction change as it sweeps around from the annular passageway between the purge sleeve and outer wall of the still tube. The danger with establishing this type of flow structure within the purge system is that it can draw contaminants through down into the still tube that will eventually deposited onto the pyrometer lens resulting in lens fouling.

Analysis of Particle Trajectories

Using FLUENT's builtin particle tracking capabilities, particles were injected into the purge airflow to determine the level of particle

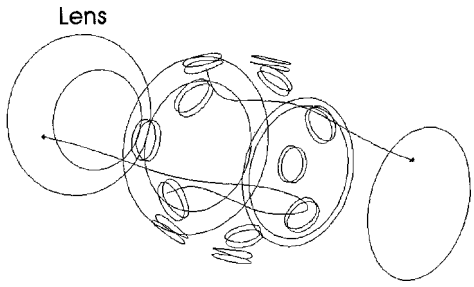

Fig. 12 Particle tracks for purge air deposition analysis.

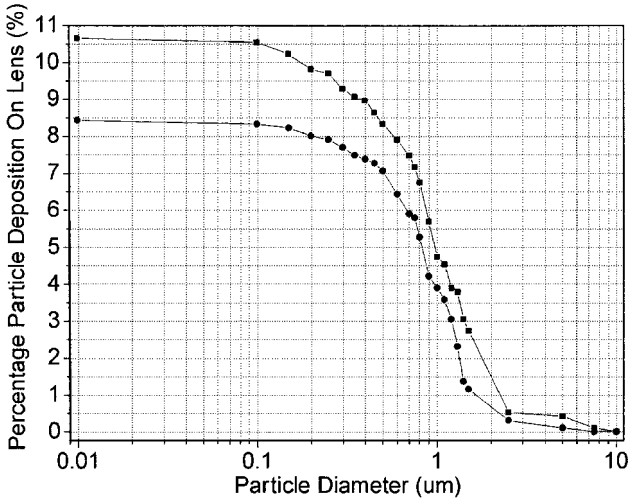

Fig. 13 Level of purge air deposition: ■, cruise and ●, maximum thrust.

deposition onto the surface of the pyrometer lens due to both purge air deposition and turbine chamber penetration. The level of deposition on the lens was evaluated in terms of the percentage particle deposition as defined by

$$\text{percentage particle deposition} = \frac{\text{particles deposited on lens}}{\text{particles injected into purge}} \times 100 \quad (1)$$

Consider, first, the fouling due to contaminant particles in the purge air. Ideally such particulates should remain entrained in the airflow and exit the purge system (Fig. 12). However, certain particles can become drawn into the still tube due to the swirling pattern at the still tube mouth and then impact with the lens (Fig. 12). An analysis of the level of particle deposition vs particle diameter was conducted, through CFD modeling at both the cruise and maximum thrust conditions, and the results are presented in Fig. 13. Figure 13 shows that there are essentially three regions that have a contribution to purge air deposition. First, with particles having a diameter smaller than 0.1 μm, there is a constant level of deposition of approximately 10.5% at cruise and 8.5% at maximum thrust. This is because these smaller particles have a tendency to remain entrained with the airflow and, therefore, a fixed portion will become captured by the swirl at the still tube mouth such that they then impact the lens. The level of deposition is lower at the maximum thrust condition because the purge inlet pressure is greater and, thus, the particles have a higher inertia. Second, there is a sigmoidal transition region between 0.1 and 10 μm whereby the number of particles depositing on the lens decreases with particle diameter. Finally, particles greater than 10 μm have such a high inertia that they do not swirl around into the still tube and, therefore, have a negligible effect on lens fouling. It was also found that of those particles injected through the purge air inlets that deposit on the lens there is an approximate split of 39% vs 61% contribution to fouling from particles through the first row of purge air inlets compared to the second row (Fig. 14). In the case of the RB199, purge air deposition is primarily responsible for the level of pyrometer lens fouling.

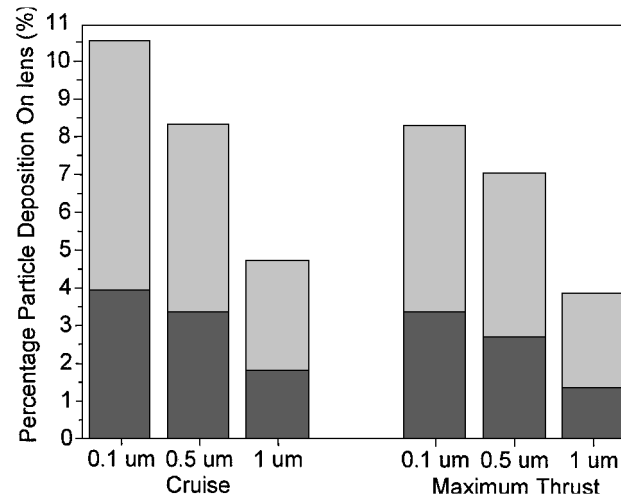

Fig. 14 Contribution of fouling due to purge inlets: ■, row 1 and ■, row 2.

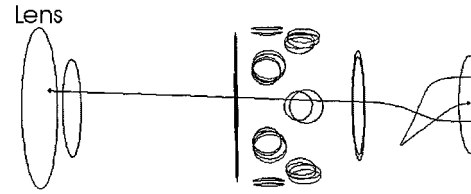

Fig. 15 Particle tracks for turbine chamber penetration.

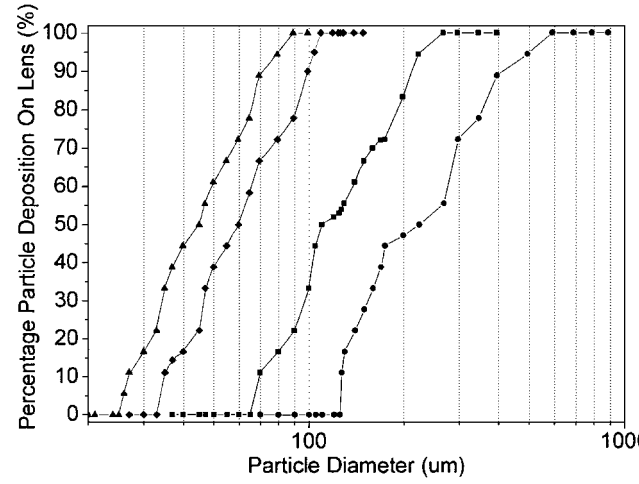

Fig. 16 Level of turbine chamber penetration: ■, 50 m/s at cruise; ●, 50 m/s at maximum *T*; ▲, 100 m/s at cruise; and ♦, 100 m/s at maximum *T*.

Consider next the level of optical contamination due to turbine gas path particles penetrating the pyrometer sight tube; ideally the purge airflow should redirect any particulates back into the turbine chamber as shown in Fig. 15a. However, certain particles with a high enough inertia can shoot directly up through the sight tube and into the still tube to impact with the lens as shown in Fig. 15b. Analysis of the level of particle deposition vs particle diameter due to turbine chamber penetration, at two different initial particle velocities, was conducted, at both the cruise and maximum thrust engine conditions, and the results are presented in Fig. 16. Figure 16 shows that there are three regions that contribute to the problem of lens fouling. First, for each sigmoidal curve of initial particle velocity, there is negligible deposition below a specific particle diameter. For instance, at the cruise condition with particles penetrating the sight tube with an initial velocity of 50 m/s, particles having a diameter less than 65 μm are completely redirected back out of the sight tube because they do not have enough inertia to overcome the opposing

purge airflow. Second, there is a transition region through a range of particle diameters whereby the number of particles that have the ability to impact and, thus, deposit on the lens increases with increasing particle diameter. Finally, there is a minimum particle diameter above which, for a given initial particle velocity, a particle has such a high degree of inertia that it can completely penetrate the purge air system and impact the lens. In the case of particles with an initial penetrating velocity of 50 m/s at engine cruise, this diameter is 300 μm (Fig. 16).

Summary

The predominant flow feature within the RB199 pyrometer purge air system is the significant recirculation, or swirl, of the purge air in front of the still tube mouth. Once this swirl pattern is developed, a subsequent negative flow is established into the core of the still tube. This motion will significantly increase the likelihood of contaminants coming in contact with the lens surface and depositing to result in optical fouling of the instrument's optics. From the analysis of particle tracking, through CFD, it was shown that for contaminants in the purge airflow having a diameter of less than 0.1 μm a constant level of deposition of approximately 10.5% at engine cruise and 8.5% at maximum thrust is produced. For particles in the transition region between 0.1 and 10 μm, the level of fouling due to purge air deposition decreases sigmoidally with increasing diameter. Particles greater than 10 μm diameter were found to have a negligible effect on lens fouling because such particles have a high inertia and, therefore, do not swirl around into the core of the still tube. For gas path particles that penetrate the pyrometer sight tube, from the turbine chamber, it was found that there was negligible deposition below a specific particle diameter for a given initial particle velocity, with the particles being completely redirected back out of the sight tube. There is also a transition region through a range of particle diameters whereby the number of particles that have the ability to impact and, thus, deposit on the lens increasing with increasing particle diameter. Finally, there is a minimum particle diameter above which, for a given initial particle velocity, a particle has such a high degree of inertia that it can completely penetrate the purge air system and impact the lens, resulting in contamination of the pyrometer lens. In the case of the RB199 installation, purge air deposition is primarily responsible for the level of pyrometer lens fouling.

Acknowledgments

The authors would like to acknowledge the U.K. Engineering and Physical Sciences Research Council and Rolls–Royce, plc. as project sponsors and to thank C. Bird and P. Loftus for the guidance received during the course of this study.

References

[1]Kerr, C., and Ivey, P., "An Overview of the Measurement Errors Associated with Gas Turbine Aeroengine Pyrometer Systems," *Measurement Science and Technology*, Vol. 13, No. 6, 2002, pp. 873–881.

[2]Rohy, D. A., Duffy, T. E., and Compton, W. A., "Radiation Pyrometer for Gas Turbine Engines," Society of Automotive Engineers, SAE Paper 720159, 1972.

[3]Graham, H., "Use of Existing Maintenance Data to Evaluate the Impact of Engine Technologies on the Installed Life of the Turbo Union RB199," M.S. Thesis, School of Mechanical Engineering, Cranfield Univ., Cranfield, England, U.K., 2000.

[4]Davinson, I., "Conversion of Turbine Blade Pyrometer Output Voltages into Temperatures," Rolls–Royce, Ltd., Rept. EIR00880, Derby, England, U.K., 1984.

[5]Wheatley, B. J., "Turbine Blade Pyrometry Versus Thermocouples—Effects on Lifing and Performance," M.S. Thesis, School of Mechanical Engineering, Cranfield Inst. of Technology, Cranfield, England, U.K., 1989.

[6]Senior, K. S., "Development of a Desktop Analytical Method for Determining Thrust Degradation in Installed Military Turbofans," M.S. Thesis, School of Mechanical Engineering, Cranfield Univ., Cranfield, England, U.K., 1999.

[7]Kerr, C. I., and Ivey, P. C., "A Review of Purge Air Designs for Aeroengine Based Optical Pyrometers," *Journal of Turbomachinery*, Vol. 124, No. 2, 2002, pp. 227–234.

[8]Kirby, P. J., "Some Considerations Relating to Aero Engine Pyrometry," *Advance Instrumentation for Aero Engine Components*, CP-399, AGARD, May 1986.

[9]Sellers, R. R., Przirembel, H. R., Clevenger, D. H., and Lang, J. L., "The Use of Optical Pyrometers in Axial Flow Turbines," AIAA Paper 89-2692, July 1989.

[10]Berenblut, B. J., and Masom, R. A., "Radiation Pyrometry for Gas Turbine Engines—An Introduction," *The British Journal of Non-destructive Testing*, Vol. 24, No. 5, 1982, pp. 268, 269.

[11]Hayden, T., Myhre, D., Pui, D. Y. H., Kuehn, T. H., and Tsai, C. J., "Evaluating Lens Purge Systems for Optical Sensors on Turbine Engines," AIAA Paper 88-3037, July 1988.

[12]Brocklehurst, H. T., "Soot and Radiation Modelling in Gas Turbine Combustion Chambers," Eng.D. Dissertation, School of Mechanical Engineering, Cranfield Univ., Cranfield, England, U.K., 1997.

[13]Lefebvre, A. H., *Gas Turbine Combustion*, 2nd ed., Taylor and Francis, New York, 1999.

[14]Koylu, U. O., Faeth, G. M., Farias, T. L., and Carvalho, M. G., "Fractal and Projected Structure Properties of Soot Aggregates," *Combustion and Flame*, Vol. 100, No. 4, 1995, pp. 621–633.

[15]Smedley, D. A., "Line Loss Corrected Aerotrace Smoke Particulate Data," Rolls–Royce, plc., Rept. DNS 40811, Derby, England, U.K., 1997.

[16]Fisher, E. A., and Lewis, T. J., "Experimental Pyrometer System for a Gas Turbine Engine," AIAA Paper 92-3482, July 1992.

[17]Myhre, D. C., Pui, D. Y. H., and Miller, L. V., "Purge Air System for a Combustion Instrument," U.S. Patent 4,786,188, Rosemount, 1988.

[18]Sage, W., "The Erosive Characteristics of Natural Sands and Abrasive Dusts," National Gas Turbine Establishment, Rept. NT699, Ministry of Technology, Pyestock, England, U.K., 1968.

[19]Moorcroft, G., "Investigations of Algerian and Saudi Arabian Desert Sands," Rolls–Royce Ltd., Rept. ESL19071, Derby, England, U.K., 1981.

[20]Kerr, C. I. V., "The Effect of Purge System Design on the Application of Optical Pyrometry to Aeroengines," Eng.D. Dissertation, School of Engineering, Cranfield Univ., England, U.K., 2002.